Bull. Astr. Soc. India (1982) **10**, 187–196.

NOTES FOR THE OBSERVER

by T. P. Prabhu

1. Astronomical photography

Last three decades of astronomical photography have seen a great improvement in the detective performance and standardization of the photographic emulsion. The use of computers to analyze the data converted to the digital form by the modern microphotometers has made it possible to extract the maximum information from the images stored in the photographic medium. While the precision of the photographic photometry was limited to about 10 per cent a few decades ago, it is now possible to exceed a precision of 1 per cent over a large range of photographic densities. The maximum utilization of the photographic emulsion is possible only through the quantification and standardization of the photographic response.

The photographic response

The light incident on the photographic plate forms a *latent image* which, on developing, is reduced to dark grains of silver. The image is stored—after the process of fixing—in the form of blackening. The degree of blackening depends on the amount of light incident on an individual element of the photographic emulsion. Once the plate is calibrated with the incident light intensity as a function of the degree of blackening, the image stored in the emulsion can be converted back to the light intensity as a function of position. To this end, one must first standardize the measures of the photographic response and the incident light.

The degree of blackening is generally measured as *density*

$$D = -\log_{10} T$$

where T is the transmittance of the region of the photographic plate under investigation. If I_0 is the intensity of light incident on the photographic record and I_t is the intensity transmitted by it, the transmittance T is defined as the fraction I_t/I_0. The photographic response is generally calibrated in terms of a *characteristic curve* which expresses D as a function of E or inversely E as a function of D. $D = F(E)$ may be determined in the laboratory and inverted to $E = F(D)$. The latter is used to convert the image stored photographically into one that is physically meaningful. The curve, $D = F(E)$ was first used by Ferdinand Hurter & Vero Driffield in 1908, and is generally known as H and D curve.

The calibration of a photographic plate involves exposing it to different known values of intensity, measuring the transmission values at these different levels and drawing a curve between the transmission and the intensity. Generally, one is satisfied with the relative intensities. Thus, the intensity is varied by a known amount of attenuation using for example a set of neutral-density filters. Since the photographic

plate records the total amount of light received by it (*i.e.* exposure = intensity × duration of exposure), one may keep the intensity constant and vary the exposure time. The transmittance is measured using a microdensitometer (more precisely, a microphotometer). This instrument passes a collimated beam of light through a photographic record and measures the transmitted light. The unexposed part of the emusion is generally taken as the *zero-point* (100 per cent transmission, or $T = 1$). A calibration curve is generally drawn between percentage transmission and the relative exposure. If one measures the percentage transmission of an element of the photographic image of interest, one may read the relative exposure—and hence the relative intensity—off the calibration curve.

The nature of the characteristic curve is known to depend on various factors even for the same combination of emulsion and developer. These factors include the exposure time, the wavelength of radiation and the conditions of developing. Thus, in order to obtain the most accurate results, the exposure time and the wavelength of light to which the calibration plate is exposed are matched as precisely as possible with the similar quantities related to the photographic record of interest. Further, the two plates are developed together so that the conditions during processing remain identical. Also, the calibration is registered on a piece of the same plate or film on which the image being studied is photographed. Quite often one registers the calibration image on the same plate at an auxiliary calibration set-up at the end of an observation. Spectrographs have been designed with the calibration set-up attached to them so that the calibration exposure can continue on a part of the plate simultaneously while the stellar spectrum is being recorded.

Standardization of the characteristic curve

While the above treatment of the calibration curve is sufficient for the reduction of a photographic image to relative intensity units, greater care is necessary to make an intercomparison of photographic plates used at different observatories with different calibration equipment and different microphotometers. The American Astronomical Society's working group on photographic materials in astronomy (AAS-WGPM) and the Eastman Kodak company have joined hands in standardizing the methods used in photographic photometry. Most of their recommendations and results are published in the AAS Photo-Bulletin. D. W. Latham and A. A. Hoag have contributed immensely towards the procedure of standardization.

The standardized amount of light is measured through *exposure E*. defined as the number of photons incident over an area of $1000\mu m^2$ with a specified exposure time and a specified effective wavelength of the incident light. The specification of exposure time is necessary because of the effects of reciprocity failure. The photographic response depends on the colour of the incident light too.

The zero-point of the transmission scale is defined with the plate removed from the measuring beam (and the microphotometer refocussed) instead of the conventional *clear* portion of the photographic plate. Further, the ANSI *diffuse* density scale is recommended. When a collimated beam is passed through the photographic plate, a part of the light is absorbed by the grains and a part transmitted. Only a

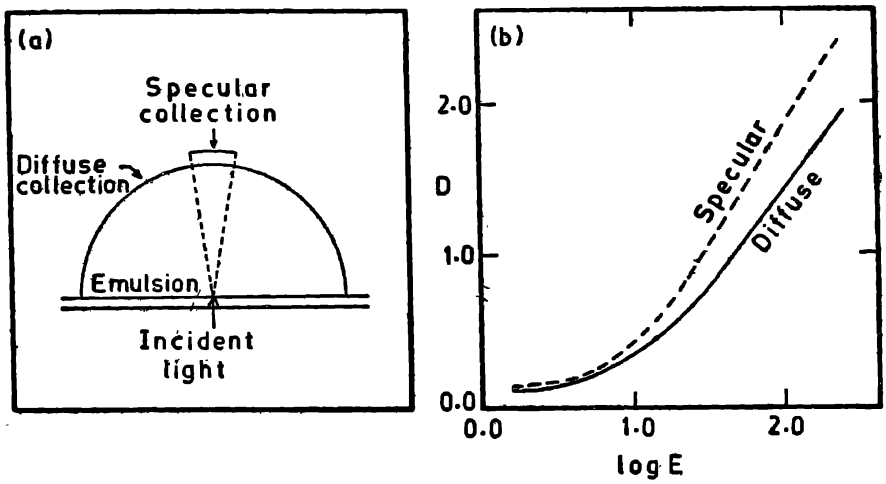

Figure 1. (a) Schematic representation of the microphotometer. The microphotometers which collect light only over a small angle yield specular densities while the ones which collect all the transmitted light yield diffuse densities. (b) Schematic characteristic curves for specular and diffuse densities. The specular densities are darker and reach saturation quicker. The difference between the two densities decreases for a finer grain-size of the emulsion.

fraction of the transmitted light continues in the same direction and the remaining is scattered over 2π steradians (figure 1a). Conventional microphotometers collect only a part of this light depending on the size of the objective and its distance from the photographic plate. The density derived from such a microphotometer is called the *specular density*. Special microphotometers have been built which collect almost the entire light scattered in 2π steradians. The density derived with the help of such instruments is the *diffuse density*. Figure 1b shows schematically the characteristic (D–log E) curves derived using the two types of densities. The difference between the specular and diffuse densities reduces as the granularity of the emulsion decreases.

Linearizing the characteristic curve

One of the shortcomings normally ascribed to the photographic emulsions is that its response to the incident light is not linear. The characteristic curve expressed as T–log E or D–log E curve is characterized by a toe (where the light intensity is not sufficient to reduce the silver), a linear part and a shoulder (where the saturation begins). The D–log E curve is linear over a longer range of response than the T–log E curve. While the T–log E curve begins to saturate around $T = 0.1$ ($D = 1$), the D–log E curve continues to be linear till densities close to 2. The general shape of the curve is similar in both the cases and defies curve-fitting with any simple formula. A. E. Baker in 1925 therefore proposed a modification of the definition of density as

$$D_1 = \log_{10}(10^D - 1) = D + \log_{10}(1 - 10^{-D}).$$

With this definition, the toe of the D_1–log E curve disappears and the characteristic curve stays linear over a large range. Baker-transformed densities were long

forgotten till G. de Vaucouleurs (1968, *Applied Optics* 7, 1513) rediscovered it. De Vaucouleurs defined *opacitance* as

$$\omega = \frac{1}{T} - 1,$$

whence we obtain $D_1 = \log \omega$. de Vaucouleurs suggests a name *densitance* for the density D_1. The log ω–log E curves are highly linear with a slope between 0.4 and 0.7 for most of the astronomical emulsions.

While the most obvious advantage of a linear log ω–log E curve is the relative ease in curve-fitting, it is not the most important one. The local errors, and also most of the common systematic errors encountered in the technique of calibration introduce a nonlinearity in the log ω–log E curve. With a little experience one can trace the cause of such effects and eliminate them from the techniques employed in the calibration process. The normal H–D curve does not have this advantage. The local and the systematic errors stand out better in the curve that employs the Baker-transformed densities. That is why this new definition of the density has come into widespread use in the recent years. Figure 2 shows characteristic curves in percentage transmission, D–log E as well as on a log ω–log E representation.

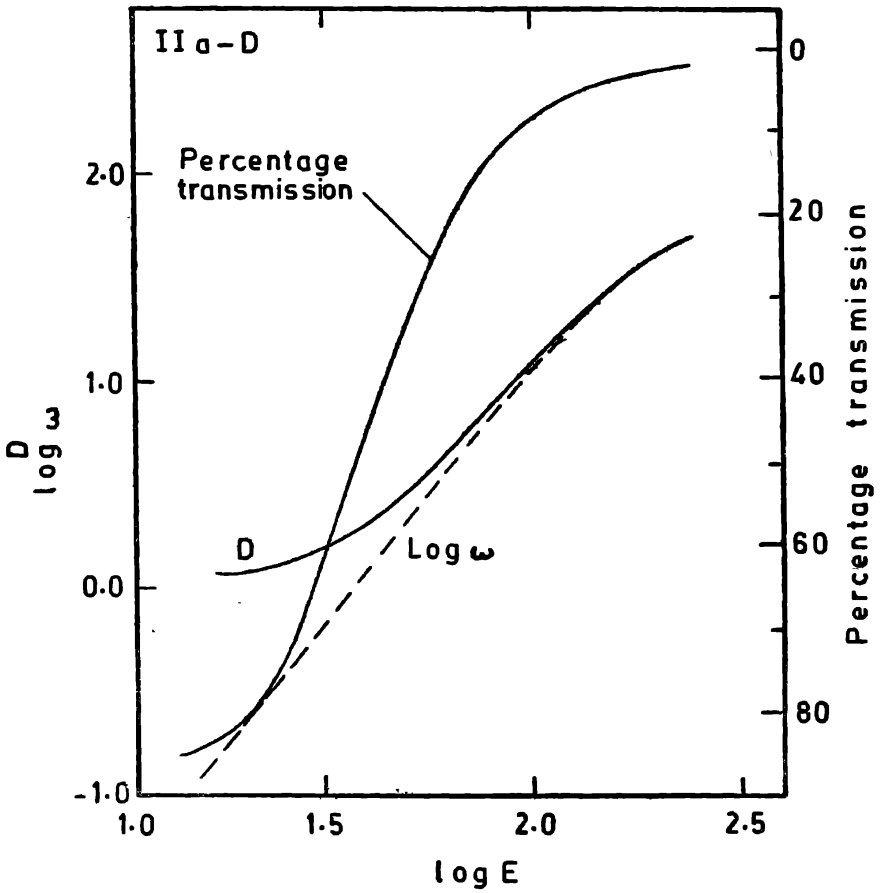

Figure 2. A typical characteristic curve of an astronomical emulsion plotted in three different representations. The percentage transmission curve is useful only for intermediate densities while the standard H–D curve can be used at higher densities also. The log ω curve is similar to the H–D curve at higher densities while it is highly linear at low and intermediate densities. The non-linearity that remains at higher densities is of microphotometer origin—especially due to the use of specular densities.

2. Mira variables

Mira-type variables are the regular long-period variables with large amplitudes (> 2.5 mag) as distinguished from the ones with shorter amplitudes as also the other forms of variable late-type giants like the irregular and semi-regular variables. Mira variables exhibit a fascinating range of astrophysical phenomena. Nevertheless they are not studied well enough. The vastness of the range of phenomena hampers a theorist. For an observer the difficulties arise because the periods are very long—over a year in the mean—and almost all their properties are time-dependent. The light curve does not repeat itself, the periodicity shows secular as well as abrupt changes and the spectroscopic changes accompanying the pulsation do not repeat exactly from one cycle to another. Thus an observational program on Mira-type variables requires observations by a group of astronomers utilizing all the different techniques of observations simultaneously. The program also needs to extend over several years.

The atmosphere of a Mira-type star is extremely tenuous. Thus, one looks at different depths at different wavelengths. Further, there may not be a precisely defined boundary of the atmosphere at all. The atmosphere smoothly joins the *circumstellar shell* which gives rise to the low-excitation absorption lines and also the infrared emission. The radius of a Mira-type star is thus extremely ill-defined; the value derived depends on the method used and the wavelength of the radiation. Several Mira-type variables are accessible for a direct measurement of sizes from the lunar occultation data. Some may even be recorded by speckle interferometry. Since one has no control over the motion of the moon, it will take a long time to compile a *radius curve* as a function of phase of the light curve for a single variable by occultation techniques even for a given wavelength of observation. There has been a variety of wavelength bands used by the same or different teams of observers thus rendering it difficult to intercompare two values of radii derived at different phases. Some standardization of the wavelength band is indeed necessary. On the other hand, the radii at different wavelengths for a given phase may be of more interest than the radii at the same wavelength at different phases. The former would help us to understand the stratification in the envelopes of these stars. Such studies of non-variable giants and supergiants are already being carried out by the lunar-occultation as well as the speckle-interferometric techniques. The first such measurement was due to R. Hanbury Brown and associates (1970, *M. N. R. A. S.* **148**, 103) who found—using intensity interferometric technique—that the radii of the Wolf-Rayet star γ^2 Velorum is 5 times larger in the light of C III-C IV complex at λ 4650 Å, as compared to the radius in the blue light.

High dispersion spectroscopy of Mira-type variables has shed more light in the recent years on their atmospheric stratification. The spectra of Mira-type variables are extremely rich in information. They contain the atomic absorption lines in the blue and the absorption lines due to the metallic oxides in the visual and near-infrared Hydrogen lines from Balmer to Brackett series appear in emission just before maximum light and continue to be seen until near minimum. The region beyond 1.5 μm is rich with the rotation-vibration lines of CO and H_2O. The OH maser emission and/or the thermal SiO emission may be present in the microwave region. Different lines are formed in different atmospheric layers which move with

different velocities. Thus the first step towards an understanding of the Mira atmospheres is through an investigation of the velocities of different kinds of lines. Significant progress has been achieved since H. Maehara's study (1968, *Publ. Astr. Soc. Japan* **20**, 77) of the phenomenon of doubling of atomic lines in the near-infrared. The blue component of these lines is formed in the deeper warmer layers and the red component in the outer cooler layers. Such doubling has also been observed in the absorption spectra of CO and H_2O in the near-infrared. A study of these spectra enables one to construct the models of the shock-heated gas rising through the cooler layers. The best model to date is the model of R Leonis due to K. H. Hinkle and T. G. Barnes (*Ap. J.* **220**, 210; **227**, 923; **234**, 548). More high-resolution spectroscopic data and a direct determination of radii at different wavelengths should improve our understanding of the atmospheres of Mira variables.

Figures 3, 4 and 5 present charts for three long-period variables X Centauri, R Corvi and R Hydrae, respectively. X Centauri varies between 8.0 mag and 13.4 mag on an average with a period of 314.9 days. Occasionally, it may become as bright as the seventh magnitude at maximum. It was discovered by Mrs Fleming in 1895 while examining the spectra obtained as a part of the Henry Draper program. X Centauri is 4° north of the $4\frac{1}{2}$ mag star B Centauri and 7° south of equally bright β Hydrae. The next maximum is expected in the beginning of August.

R Corvi was the first variable to be discovered in Corvus. It was listed as a ninth magnitude star by Lalande in 1796 while Argelander found it to be 7.8 mag in 1851. Karlinski in 1867 tried to use it as a comparison star for the minor planet Eunomia and could not find any star brighter than 10 mag near the expected position. Winnecke followed it the same year and confirmed its variability. Schönfeld observed the maximum of R Corvi for the first time on 1868 May 11 at 7.1 mag and a brighter one at 6.8 mag on 1869 March 26. R Corvi varies between 7.5 mag and 13.8 mag with a period of 316.9 days, an occasional maximum reaching even 6.7 mag. The next maximum is expected in the middle of December. R Corvi is situated near the centre of the constellation, at the intersection of the lines joining β Corvi to γ Corvi and δ Corvi to ε Corvi. It belongs to a class of long-period variables characterized by the absence of OH emission at 1612 MHz and 1667/65 MHz.

R Hydrae is one of the brightest long-period variables at maximum. At 10 minutes east of the $3\frac{1}{2}$ mag star γ Hydrae, it rivals the latter at some maxima. The average light variations are between 4.5 mag and 9.5 mag with a period of 388 days. It is already at maximum in June. Discovered by J. P. Maraldi in 1704, R Hydrae has held an interest over the following centuries not only because of its high peak brightness, but also because of its continuously decreasing period. The period has changed from 500 days at the time of discovery to 388 days in the recent years. Its amplitude of light variations also tends to increase. A similar decrease in the period is observed in R Aquilae (5.7 mag – 12.0 mag) which has changed its period from 320 days in 1915 to 284 days in recent years. P. R. Wood (1975, *I. A. U. Coll. No.* 29 : *Multiple Periodic Variable Stars, Invited papers*, p. 69) proposed that these stars are possible examples of stars undergoing rapid luminosity decrease following the helium shell flash in the helium burning stage. He calculated the timescales of 1200 yr and 550 yr for the luminosity decrease in R Hydrae and R Aquilae respectively which are consistent with the theoretical predictions. R Hydrae is also a maser source of SiO line at 43.122 GHz.

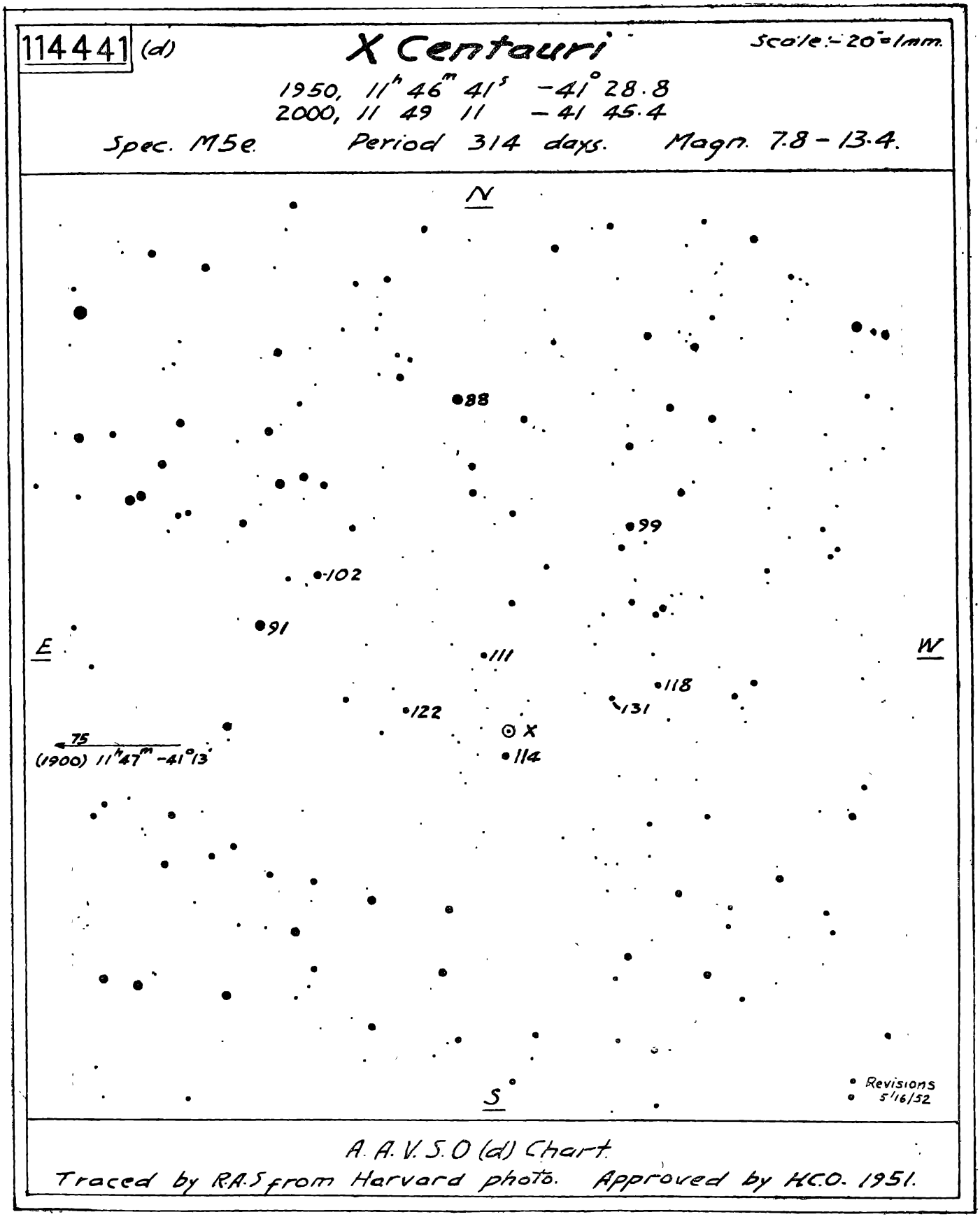

Figure 3. Identification chart for X Centauri. (Courtesy: AAVSO.)

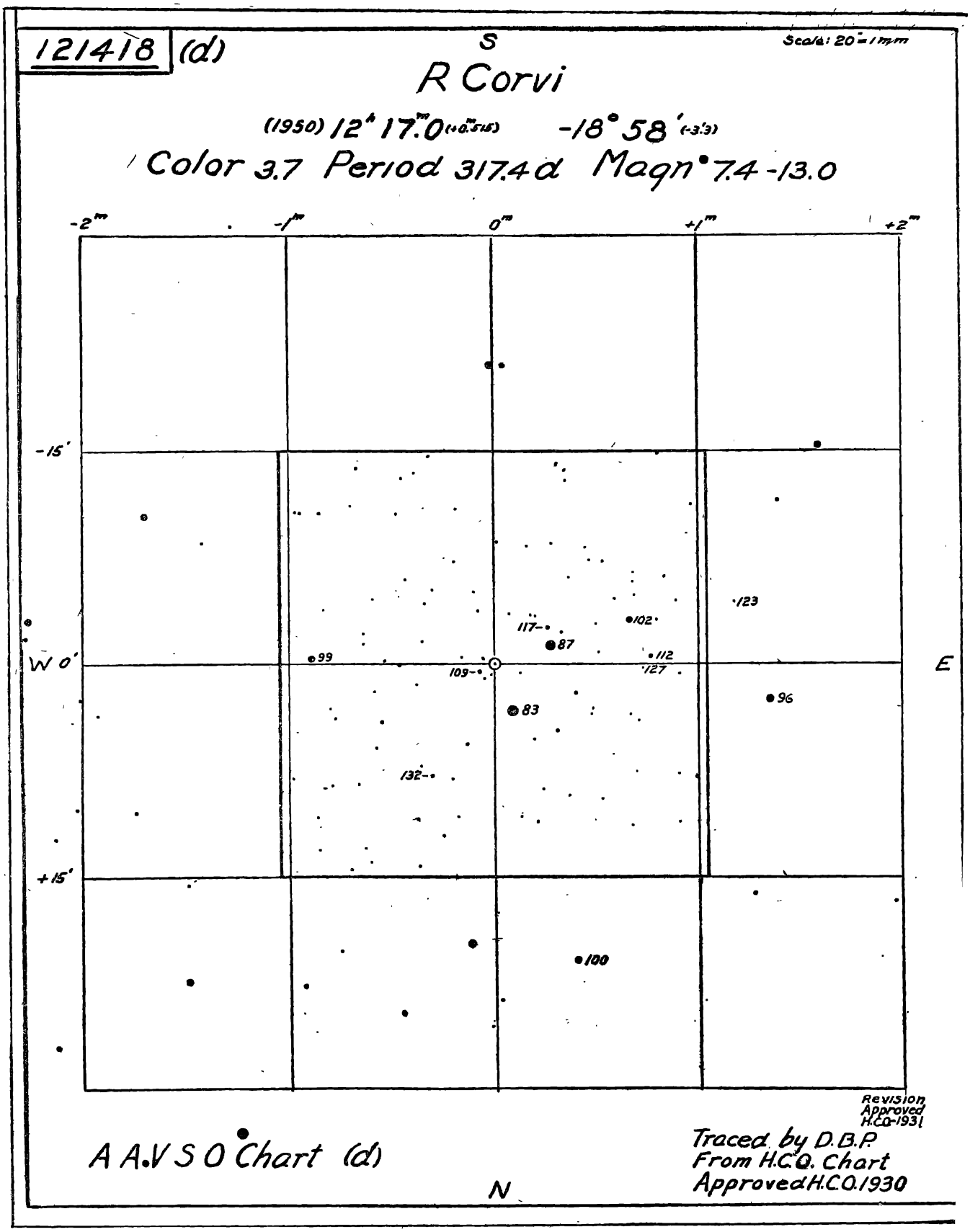

Figure 4. Identification chart for R Corvi. (Courtesy : AAVSO.)

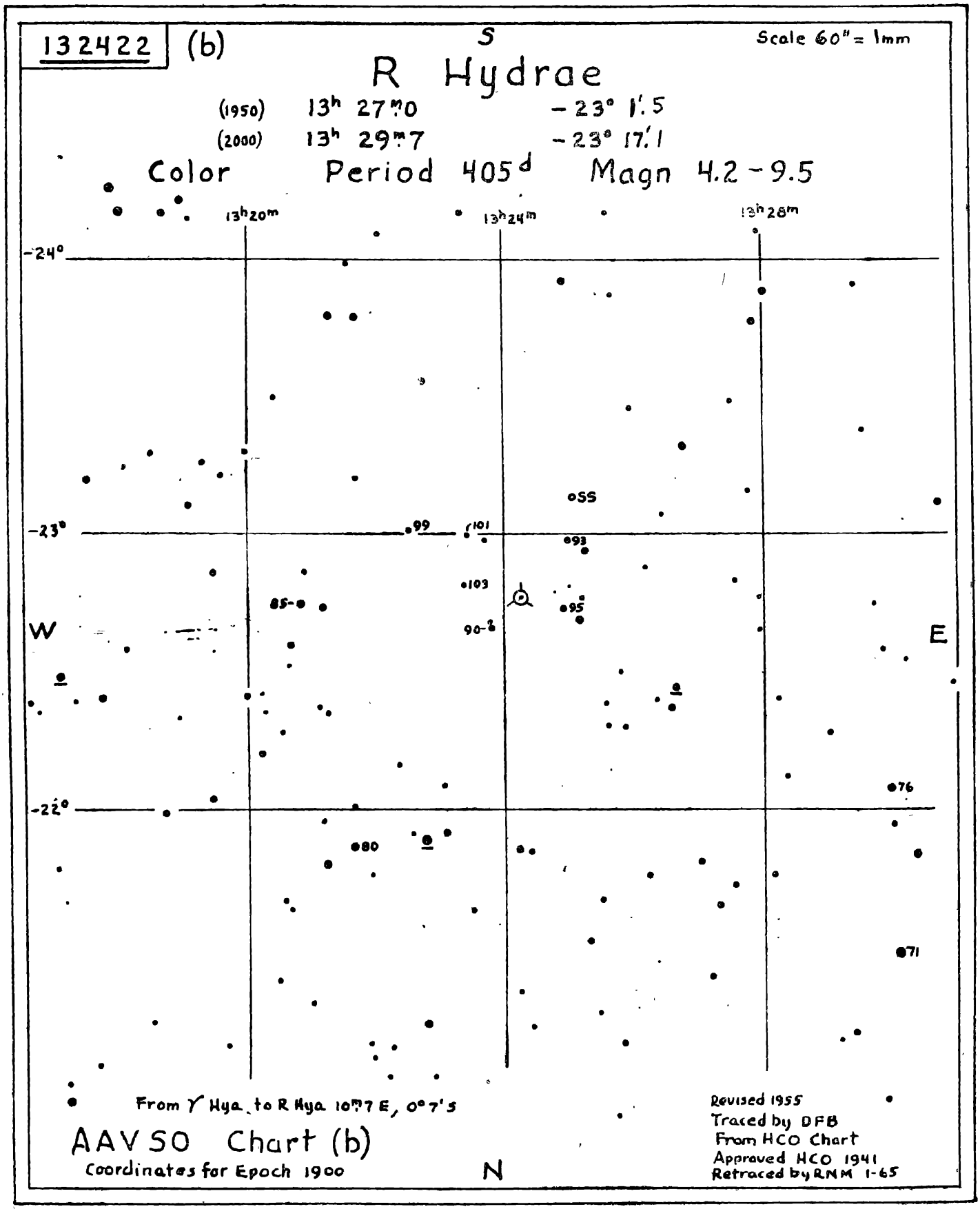

Figure 5. Identification chart for R Hydrae. (Courtesy : AAVSO.)

Table 1. Lunar occultations of bright stars predicted for Kavalur between 1982 June and October

Date		UT h	m	s	Event	Star	Mag.	Sp. T.	Altitude	Percentage illumination
June	5	17	34	45	D	HR 6053	6.4	gK2	58	99+
	22	13	34	7	D	R Geminorum	5.9-14.1	S	9	2+
		14	6	43	R				8	
July	3	19	41	11	D	HR 6269	5.9	dG3	37	94+
	18	23	53	40	D	HR 2169	6.0	gK4	15	4—
August	14	20	46	46	D	ζ Tauri	3.0	B2 IVp	4	23—
		21	5	27	R				8	
		21	37	46	D	HR 1929	6.3	A2 V	15	23—
		22	13	6	R				24	
	28	18	5	16	D	HR 6716	5.7	B0 Ib	24	71+
	29	19	30	58	D	HR 7128	5.9	B8	17	80+
September	6	22	19	46	D	ν Piscium	4.7	K3 III	74	87—
		23	10	50	R				62	
	11	20	54	38	D	μ Geminorum	3.2	M3 III	30	36—
		21	36	14	R				35	
	27	17	16	58	D	4 Capricorni	6.0	G8 IV	38	73+
	30	20	29	0	D	74 Aquarii	5.9	B9	33	94+
October	1	23	29	55	D	HR 9014	6.3	gK4	4	98+
	28	12	53	7	D	HR 8836	6.4	K5	44	82+
		17	16	26	D	ψ^3 Aquarii	5.2	A0 V	57	83+
	30	21	9	5	D	26 Ceti	6.2	dF0	30	96+

3. Lunar occultations

Bright stars occulted by the moon—as seen from Kavalur—between 1982 June and October are listed in table 1. The reappearance is listed only when the disappearance is also observable. R Geminorum occults on June 22 and is a long-period variable of 369.9 d period. It would fortunately be close to its maximum at the time of occultation. The twilight and the low altitude of the moon would make this occultation somewhat difficult to observe. ζ Tauri is a shell star and it would be interesting to observe its occultation simultaneously in H_α and in continuum light. Similar observations of the M supergiant 119 Tauri were carried out by N. M. White, T. J. Kreidl and L. Goldberg (1982, *Ap. J.* **254**, 670) who demonstrated that the region in which the absorption line of H_α is formed is at least twice as large as the region which emits the continuum light. The galactic cluster M 21 will be occulted by the moon on August 28 at $14^h\ 59^m\ 39^s$ UT. The individual stars in this cluster are fainter than 9 mag, though about 40 are brighter than 12. The altitude of the moon would be very low at the time of the occultation. Two minor planets are also being occulted by moon in the forthcoming months. 20 Massalia (11.5 mag) will be occulted on August 28 at $14^h\ 29^m\ 46^s$ UT, and 145 Adona (12.4 mag) will reappear from the dark edge of moon on October 9 at $20^h\ 15^m\ 35^s$ UT. These events would last about a second.